Robust paths to net greenhouse gas mitigation and negative emissions via advanced biofuels

John L. Field[a,1,2], Tom L. Richard[b], Erica A. H. Smithwick[c,d], Hao Cai[e], Mark S. Laser[f], David S. LeBauer[g], Stephen P. Long[h,i,j], Keith Paustian[a,k], Zhangcai Qin[e,l,m], John J. Sheehan[n,o], Pete Smith[p], Michael Q. Wang[e], and Lee R. Lynd[f,1]

[a]Natural Resource Ecology Laboratory, Colorado State University, Fort Collins, CO 80523; [b]Department of Agricultural and Biological Engineering, The Pennsylvania State University, University Park, PA 16802; [c]Department of Geography, The Pennsylvania State University, University Park, PA 16802; [d]Earth and Environmental Systems Institute, The Pennsylvania State University, University Park, PA 16802; [e]Energy Systems Division, Argonne National Laboratory, Lemont, IL 60439; [f]Thayer School of Engineering, Dartmouth College, Hanover, NH 03755; [g]Arizona Experiment Station, University of Arizona, Tucson, AZ 85721; [h]Department of Crop Sciences, University of Illinois at Urbana–Champaign, Urbana, IL 61801; [i]Lancaster Environment Centre, Lancaster University, LA1 4YQ Lancaster, United Kingdom; [j]Department of Plant Biology, University of Illinois at Urbana–Champaign, Urbana, IL 61801; [k]Department of Soil and Crop Sciences, Colorado State University, Fort Collins, CO 80523; [l]School of Atmospheric Sciences, Guangdong Province Key Laboratory for Climate Change and Natural Disaster Studies, Sun Yat-sen University, Guangzhou 510245, China; [m]Southern Marine Science and Engineering Guangdong Laboratory (Zhuhai), Zhuhai 519082, China; [n]School of Agricultural Engineering, University of Campinas, Campinas, SP 13083-875, Brazil; [o]Department of Chemical and Biological Engineering, Colorado State University, Fort Collins, CO 80523; and [p]Institute of Biological and Environmental Sciences, University of Aberdeen, AB24 3UU Aberdeen, United Kingdom

Edited by Christopher B. Field, Stanford University, Stanford, CA, and approved July 14, 2020 (received for review November 27, 2019)

Biofuel and bioenergy systems are integral to most climate stabilization scenarios for displacement of transport sector fossil fuel use and for producing negative emissions via carbon capture and storage (CCS). However, the net greenhouse gas mitigation benefit of such pathways is controversial due to concerns around ecosystem carbon losses from land use change and foregone sequestration benefits from alternative land uses. Here, we couple bottom-up ecosystem simulation with models of cellulosic biofuel production and CCS in order to track ecosystem and supply chain carbon flows for current and future biofuel systems, with comparison to competing land-based biological mitigation schemes. Analyzing three contrasting US case study sites, we show that on land transitioning out of crops or pasture, switchgrass cultivation for cellulosic ethanol production has per-hectare mitigation potential comparable to reforestation and severalfold greater than grassland restoration. In contrast, harvesting and converting existing secondary forest at those sites incurs large initial carbon debt requiring long payback periods. We also highlight how plausible future improvements in energy crop yields and biorefining technology together with CCS would achieve mitigation potential 4 and 15 times greater than forest and grassland restoration, respectively. Finally, we show that recent estimates of induced land use change are small relative to the opportunities for improving system performance that we quantify here. While climate and other ecosystem service benefits cannot be taken for granted from cellulosic biofuel deployment, our scenarios illustrate how conventional and carbon-negative biofuel systems could make a near-term, robust, and distinctive contribution to the climate challenge.

biofuels | BECCS | ecosystem modeling | life cycle assessment | negative emissions

Climate stabilization plans—particularly those that aim to limit warming below 1.5 °C—rely on land-based biological mitigation (1) from bioenergy production and terrestrial carbon sequestration as a unique and essential complement to renewable electricity deployment and other greenhouse gas (GHG) mitigation measures across all emissions sectors (2, 3). Liquid biofuel production (BP) is currently among the most technologically mature and cost-effective routes to decarbonizing aviation, shipping, long-haul transport, and residual nonelectrified light-duty transport (4, 5). In addition, bioenergy systems can contribute to large-scale carbon dioxide removal (CDR) via carbon sequestration in the soils on which feedstock crops are cultivated (depending on former land use) (6) and via bioenergy with carbon capture and storage (BECCS) (7) or biochar coproduction (8). While much BECCS assessment to date has focused on electricity-producing systems, the high-purity by-product CO_2 streams from BP do not require separation and concentration steps and thus are an efficient and low-cost target for near-term carbon capture and storage (CCS) deployment (9). Achieving significant bioenergy-based GHG mitigation at useful timescales implies a scale-up of biomass feedstock cultivation and a build-out of associated logistics, conversion, and perhaps CCS infrastructure at rapid rates (10, 11).

The underlying logic of GHG mitigation through biofuels and bioenergy production has, however, been repeatedly challenged. While material and energy inputs into BP supply chains are well studied (12), more recent critiques focus on whether feedstock crops can be sustainably sourced without causing self-defeating

Significance

The climate benefits of cellulosic biofuels have been challenged based on carbon debt, opportunity costs, and indirect land use change, prompting calls for withdrawing support for research and development. Using a quantitative ecosystem modeling approach, which explicitly differentiates primary production, ecosystem carbon balance, and biomass harvest, we show that none of these arguments preclude cellulosic biofuels from realizing greenhouse gas mitigation. Our assessment illustrates how deliberate land use choices support the climate performance of current-day cellulosic ethanol technology and how technological advancements and carbon capture and storage addition could produce several times the climate mitigation potential of competing land-based biological mitigation schemes. These results affirm the climate mitigation logic of biofuels, consistent with their prominent role in many climate stabilization scenarios.

Author contributions: L.R.L. initiated the analysis; J.J.S. and L.R.L. acquired funding; J.L.F., T.L.R., E.A.H.S., K.P., and L.R.L. designed research; J.L.F. performed research; T.L.R., E.A.H.S., H.C., M.S.L., D.S.L., S.P.L., Z.Q., J.J.S., P.S., and M.Q.W. contributed new analytic tools; J.L.F. analyzed data; and J.L.F. and L.R.L. wrote the paper.

Competing interest statement: The Energy Biosciences Institute was funded by BP America, Inc.

This article is a PNAS Direct Submission.

[1]J.L.F. and L.R.L. contributed equally to this work.

[2]To whom correspondence may be addressed. Email: john.L.field@gmail.com.

This article contains supporting information online at https://www.pnas.org/lookup/suppl/doi:10.1073/pnas.1920877117/-/DCSupplemental.

First published August 24, 2020.

reductions in ecosystem carbon storage. Conversion of nonagricultural land with high initial carbon stocks to the cultivation of corn or other first-generation biofuel feedstock crops can result in large up-front ecosystem carbon storage reductions ("carbon debt") that must be overcome via subsequent fossil fuel displacement or carbon sequestration before net mitigation is achieved (13). Conversion of existing productive agricultural land with low carbon stocks can also be counterproductive if the loss of commodity production there leads to compensatory agricultural expansion (and associated ecosystem carbon losses) elsewhere, an effect known as indirect land use change (ILUC) (14). ILUC concerns may be minimized or avoided by targeting feedstock production on low-productivity or abandoned cropland (15, 16) or on land "spared" from continued agricultural use through future agricultural intensification or dietary shifts (17, 18). However, since reforestation often offers an alternative use of such land for biological mitigation, it has been suggested that bioenergy assessments should consider the "opportunity cost" of the foregone ecosystem carbon sequestration of reforestation when land is used instead for feedstock production (19).

While each of these ideas was originally applied to first-generation biofuels from food crops, critiques around carbon debt (20), ILUC (21), and opportunity costs (22, 23) have all subsequently been invoked for the production of cellulosic biomass to use in electricity generation or advanced BP. Synthesizing these and other sustainability concerns, recent studies have suggested that the dedicated use of land for bioenergy feedstock production results in suboptimal climate outcomes (24) and have recommended refocusing research efforts and policy support away from bioenergy technology toward land-based biological carbon management (25). However, those conclusions are often based on secondary estimates of bioenergy system performance and mitigation opportunity costs and generally exclude consideration of CCS or future technology improvements. Researchers have also called for more biophysically explicit assessments that establish bioenergy system mitigation in terms of increased net carbon fluxes from the atmosphere into feedstock-producing ecosystems (via either increased carbon fixation or reduced respiration, so-called "additional carbon") (26–29).

Here, we couple ecological, engineering, and life cycle emissions accounting models to estimate the biophysical potential of perennial energy grass cultivation and BP to replace fossil energy sources and to directly sequester carbon, in comparison to other land-based biological mitigation schemes. A process-based ecosystem model was calibrated to perform temporally explicit simulation of atmosphere–biosphere carbon exchanges under different land use choices at three case study sites. We conducted a factorial analysis estimating the net biophysical GHG mitigation potential of cellulosic BP considering different initial land uses (cropland, pasture, and secondary forest), energy grass yields (current and anticipated future), and biorefinery technology configurations [current biochemical conversion to ethanol, future hybrid conversion to ethanol and Fischer–Tropsch (FT) liquids, and future hybrid conversion with CCS], accounting for upstream life cycle production inputs. We compare those net biofuel mitigation potential results to that of reforestation or grassland restoration on former agricultural land or continued undisturbed growth of secondary (70-y-old aggrading) forest. The analysis shows that many, but not all, of the cellulosic BP scenarios considered achieve greater GHG mitigation potential than alternate land uses. This case study-based assessment quantifies the biophysical mitigation potential of BP systems as affected by initial land use and biorefining technology. BP economics, sustainable deployment scale, and impacts on biodiversity and other ecosystem services fall outside the scope of this analysis. We do, however, show that several bioenergy system design factors that we analyzed (initial land cover, feedstock production and conversion technology, and CCS) have substantially larger impact on system mitigation performance than previous estimates of ILUC from growing cellulosic crops.

Ecosystem Productivity and Carbon Storage

Terrestrial ecosystem carbon accounting requires differentiation between the gross rate of plant photosynthesis (gross primary production); the net rate of biomass carbon accumulation accounting for autotrophic respiration (net primary production [NPP]); ecosystem carbon storage accounting for heterotrophic respiration (R_h) in soils and fauna (net ecosystem production); and the change in total ecosystem carbon storage accounting for biotic and abiotic disturbance events, lateral losses, and harvests (net ecosystem carbon balance [NECB]) (30). Land use change (LUC) for bioenergy production or other mitigation purposes results in changes to NECB that reflect previous land use; the productivity, structure, and longevity of the subsequent vegetation; and carbon removal from periodic biomass harvest or other disturbance. While comprehensive measurement of these ecosystem carbon fluxes can be conducted in energy crop field experiments (31, 32), such accounting is rarely invoked in model-based bioenergy sustainability assessments (22). Process-based ecosystem models provide a framework for synthesizing discrete measurements of carbon stocks and fluxes over time, with mechanistic representations of ecosystem function to facilitate wider extrapolation and scenario evaluation. The DayCent model utilized here features daily calculation of NPP and carbon redistribution and respiration losses from biomass, litter, and soil carbon pools as affected by local climate; soil (edaphic) factors; vegetation productivity, structure, and phenology; and management (e.g., tillage, fertilizer application) practices (33).

Our analysis considered three contrasting case study sites in the United States east of the 100th meridian covering a range of climates (*SI Appendix*, Fig. S1) and ecosystem types, including two sites (Webster County, Iowa, and La Salle Parish, Louisiana) near the forest–grassland transition zone at the margin of the Great Plains region and an additional site (Wayne County, New York) in the eastern United States where forest is the more common natural land cover. We used DayCent to conduct 70-y forward simulations of productivity and changes in ecosystem carbon storage and soil nitrous oxide (N_2O) emissions at these sites for the conversion of cropland, pasture, and secondary forest to managed perennial energy grass (switchgrass, *Panicum virgatum*) or a natural vegetation alternative (reforestation, grassland restoration, or continued secondary forest growth) (*SI Appendix*, Fig. S2). We calibrated DayCent to best match carbon and nitrogen cycling observed in US switchgrass (*P. virgatum*) field trials (34) and for regionally specific secondary forest growth (35). Anticipating ongoing productivity improvements through breeding, we also modeled a "future" switchgrass variety that achieves 64% higher yield, equivalent to a 2% annual improvement compounded over 25 y. For comparison, the US Department of Energy's 2016 billion-ton report considers annual yield increase scenarios of 1, 2, 3, and 4% (36).

Fig. 1 shows ecosystem carbon cycling for the different scenarios averaged annually over the first 30 y of simulation in DayCent, a time period selected for near-term policy relevance and consistency with previous analysis (37). Simulated NPP is substantially higher for managed switchgrass cultivation (7 to 19 Mg C ha^{-1} y^{-1}) than for unmanaged reforestation or grassland restoration (2 to 7 Mg C ha^{-1} y^{-1}) on former cropland and pasture due to the higher yield potential of improved switchgrass varieties and reduced nutrient limitations after fertilizer addition (Fig. 1 and *SI Appendix*, Table S1). Our associated yield estimates for managed current-day switchgrass (10 to 14 Mg biomass ha^{-1} y^{-1}) compare well with other estimates, whereas our future switchgrass yields (16 to 22 Mg biomass ha^{-1} y^{-1}) are similar to current-day Miscanthus yields in the Midwest (38).

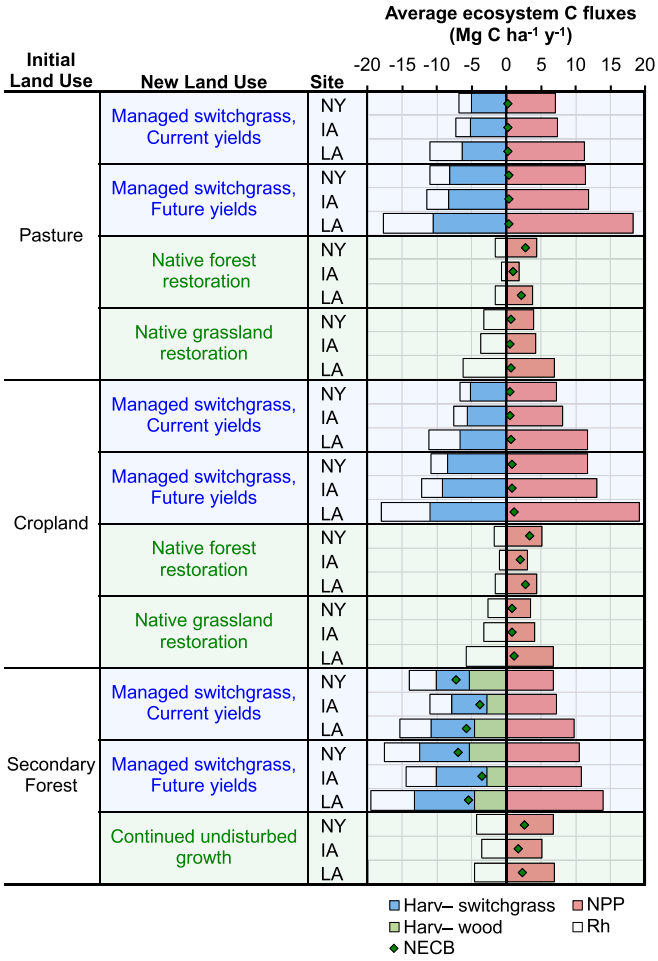

Fig. 1. Modeled ecosystem carbon fluxes for different land use scenarios. Stacked bar plot showing DayCent estimates of ecosystem carbon inputs via NPP (pink bars) and total carbon losses via both R_h (white bars) and harvest (Harv) of switchgrass (blue bars) and wood (green bars) for BP for the New York (NY), Iowa (IA), and Louisiana (LA) case studies. The resulting NECB is marked with green diamonds, with positive values indicating increases in ecosystem carbon storage. The results are annual averages across the first 30 y of simulation.

Our NECB estimates ranged from 0.1 to 1.1 Mg C ha^{-1} y^{-1} for managed switchgrass, reflecting increases in soil C stocks. Agricultural land reforestation scenarios achieved much higher NECB (1.0 to 3.4 Mg C ha^{-1} y^{-1}, corresponding on average to 61% of annual NPP), mostly through accumulation of aboveground woody biomass. Grassland restoration, in which herbaceous aboveground biomass senesces each season and only a fraction of the carbon therein is ultimately retained as litter or soil organic matter, had NECB comparable with the managed switchgrass scenarios (0.5 to 1.0 Mg C ha^{-1} y^{-1}, equivalent to 15% of NPP in those systems). In contrast, harvest of existing secondary forest and replacement with switchgrass resulted in significant net reductions in ecosystem carbon storage that persisted after 30 y (equivalent to an annualized loss rate of 3.6 to 7.2 Mg C ha^{-1} y^{-1}). These scenarios include carbon export from the system via biomass harvest (Harv), specifically from both tree biomass removal during land conversion (Harv–wood) and annual harvest of the switchgrass subsequently cultivated at the site (Harv–switchgrass). The ultimate fate of that removed biomass carbon is detailed in subsequent sections. Cumulative above- and belowground NECB for each scenario over the full course of the 70-y DayCent simulations is shown in *SI Appendix*, Fig. S3. Aboveground carbon accumulates steadily in the reforestation and continued secondary forest growth scenarios but is negligible in the grassland and switchgrass scenarios. Most scenarios show increases in belowground carbon storage, although in many cases this sequestration attenuates over the course of the 70-y simulation as soil carbon reaches a new equilibrium value.

In the switchgrass scenarios, on average 67% of seasonal NPP is harvested as biomass. Comparing across scenarios, current-day switchgrass cultivation achieves only 14% of the ecosystem carbon sequestration of reforestation ($NECB_{bfuel}$:$NECB_{veg,forest}$). However, for every megagram of reforestation carbon sequestration that is foregone in the biofuel scenario, 2.5 Mg carbon is harvested as biomass ($Harv_{bfuel}$:$NECB_{veg,forest}$). Future higher-yielding switchgrass varieties would yield 4.0 Mg biomass-C for every megagram of foregone reforestation carbon sequestration, and would achieve 0.28 Mg C of soil sequestration. Respiration losses represent a fundamental limitation on the ability of ecosystems to accumulate carbon (39), and the harvest of senesced herbaceous biomass removes carbon from the ecosystem that would otherwise largely be respired. This feedstock thus meets previously proposed system additionality requirements (25, 28).

Conversion Technology and Carbon Flows

Our analysis considered future improvements in biofuel conversion technology in addition to the increases in switchgrass yield described previously. Our "current" cellulosic biofuel technology case consisted of dilute acid pretreatment followed by simultaneous saccharification and fermentation to ethanol (40), similar to that deployed in existing commercial-scale cellulosic biorefineries. The future biofuel case considered ammonia fiber expansion pretreatment and consolidated bioprocessing to ethanol, followed by gasification and FT upgrading of fermentation residues (40, 41). In both cases, the remaining conversion by-products are combusted to meet biorefinery steam and power requirements, with any excess electric power exported to the grid. We also considered a BECCS variant of the future biofuel case in which the high-purity CO_2 streams from fermentation, syngas cleanup, and power island fuel gas cleanup (which together account for half of all feedstock carbon entering the biorefinery) (*SI Appendix*, Table S1) were dewatered, compressed, and injected into geological storage, rather than vented to the atmosphere.

We compared the biophysical GHG mitigation potential of these biofuel and BECCS scenarios (together abbreviated as "bfuel") with that of alternative scenarios of natural vegetation restoration or retention ("veg"). System boundaries and relevant flows of carbon between the atmosphere, biosphere, and geosphere are illustrated in Fig. 2. Cumulative ecosystem carbon sequestration or loss from our case study sites is described in terms of NPP, R_h, Harv, and NECB as defined previously. The carbon in harvested biomass is ultimately returned to the atmosphere as biorefinery emissions (BRE) of by-product CO_2 from conversion (which includes emissions from both fermentation and the combustion of nonfermented residues) or when emitted from a vehicle tailpipe during biofuel use (TP_{bfuel}). BP incurs additional biofuel supply chain (BSC) emissions (e.g., farm inputs and energy use, biomass transport, etc.) but avoids tailpipe emissions of fossil carbon (TP_{veg}) and gasoline supply chain (GSC) emissions (e.g., petroleum extraction, refining, and distribution) present in the vegetation restoration scenarios. In BECCS scenarios, biorefinery CO_2 emissions are instead captured and put into geologic storage (CCS). In scenarios of secondary forest conversion to switchgrass, we assumed that all initial aboveground forest biomass would be harvested and used as a bioenergy feedstock; we did not consider coproduction of timber and other durable wood products or land clearing via biomass burning alone. Indirect effects (e.g., ILUC) are not included in the direct emissions accounting described here but are explored subsequently.

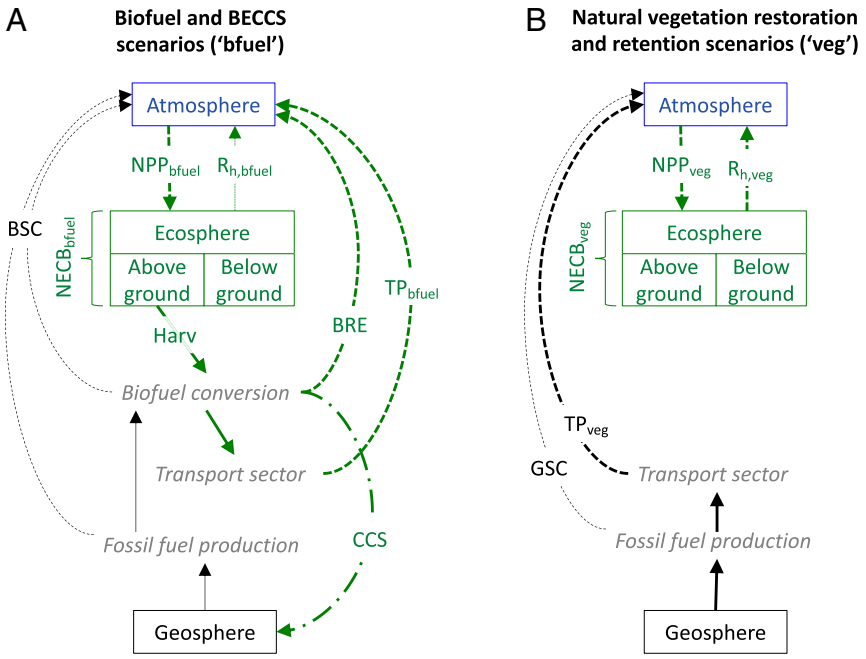

Fig. 2. Modeled atmosphere–biosphere–geosphere carbon flows. Flows of carbon between the atmosphere (blue), biosphere (green), and geosphere (black) in gaseous (dotted lines) and solid or liquid (solid lines) forms for biofuel/BECCS scenarios (bfuel; *A*) or restoration or retention of natural vegetation (veg; *B*). Geosphere-derived fossil carbon fluxes (black) include biofuel supply chain (BSC) emissions in the bioenergy scenarios and gasoline supply chain (GSC) emissions and tailpipe emissions (TP_{veg}) in the vegetation scenarios. Flows of biosphere-derived biogenic carbon (green) include NPP, R_h, Harv, biofuel combustion tailpipe emissions (TP_{bfuel}), and biorefinery emissions of by-product CO_2 (BRE), which in the BECCS scenario, are diverted into geological storage via CCS.

Land-Based Biological Mitigation Scenario Performance

We estimated the net biophysical mitigation potential (NM) of each analysis scenario by converting the simulated ecosystem carbon storage changes shown in Fig. 1 to carbon dioxide equivalent values and adding fossil fuel displacement effects, upstream supply chain life cycle impacts (agricultural inputs and farm operations, fossil fuel extraction and refining, etc.), and geological carbon sequestration via CCS (*Materials and Methods*). Fig. 3 illustrates the cumulative direct NM of the biofuel/BECCS and the natural vegetation restoration/retention scenarios over time. Mitigation is realized immediately for the conversion of former agricultural land to natural vegetation or to BP, due to increases in ecosystem carbon storage and displacement of conventional gasoline with biofuels, respectively. In contrast, secondary forest conversion to BP (using both the harvested wood and subsequently, cultivated switchgrass as feedstocks) incurs a large initial carbon deficit, which is not repaid by BP with current technology over the 70-y simulation period. Future biofuel technology requires 27 to 52 y to achieve parity with the "continued growth" forest baseline (i.e., to make up the opportunity cost of devoting that land to switchgrass production), although the addition of CCS reduces this payback period down to 6 to 8 y.

Fig. 4*A* details the average annual mitigation potential of each scenario over the first 30 y of simulation. The mitigation potential of reforestation (3.4 to 11.9 Mg CO_2e ha^{-1} y^{-1}) and grassland restoration (1.7 to 3.5 Mg CO_2e ha^{-1} y^{-1}) on former agricultural land reflects changes in NECB and ecosystem N_2O emissions, with intersite variability driven by climate, soils, plant phenology, and initial soil carbon stocks. Switchgrass cultivation on former agricultural land sequesters soil carbon at a rate of 0.5 to 3.3 Mg CO_2e ha^{-1} y^{-1}. BP also incurs benefits from avoided fossil fuel emissions (AFFE; defined as the sum of TP_{veg} and GSC). AFFE averages 7.4 and 19.9 Mg CO_2e ha^{-1} y^{-1} for the current and future cellulosic BP scenarios, respectively. This gross GHG displacement is reduced 11 to 35% by BSC and soil N_2O emissions. However, current cellulosic biofuel technology still achieves a mean NM of 6.0 Mg CO_2e ha^{-1} y^{-1} across all three sites and previous agricultural land uses (excluding the

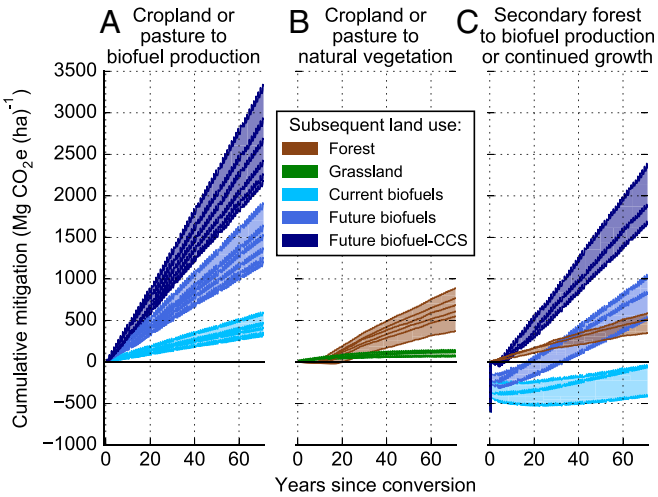

Fig. 3. Cumulative biophysical GHG mitigation potential vs. time. Results plotted individually for the three test sites under scenarios of (*A*) BP on former agricultural land, (*B*) natural vegetation restoration on former agricultural land, and (*C*) secondary forest harvest and conversion to BP vs. continued undisturbed growth. Displacement of fossil fuel emissions by BP and carbon sequestration in ecosystems or via CCS are positive mitigation; newly incurred supply chain fossil fuel emissions and ecosystem carbon losses are negative. The fine sawtooth pattern is driven by seasonal cycles of biomass growth and harvest.

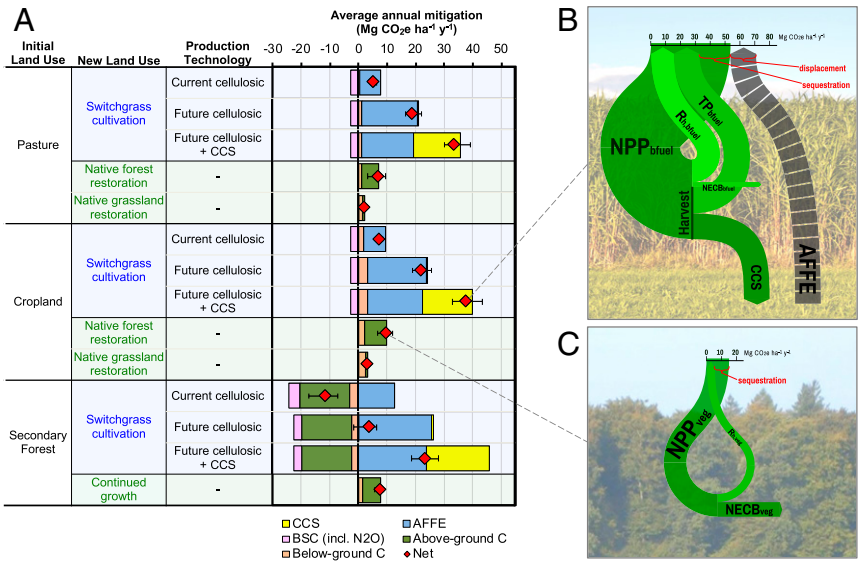

Fig. 4. (*A*) Net GHG mitigation potential for biofuel/BECCS and vegetation restoration/retention scenarios. Results are annual averages across the first 30 y of simulation for direct mitigation effects only (no ILUC or other indirect effects included). NM includes changes in above- and belowground ecosystem carbon storage, AFFE from the displacement of conventional fuel use by BP, biogenic CCS, and BSC emissions including fertilizer-derived soil N_2O emissions. Avoided emissions and carbon sequestration are positive mitigation; new fossil emissions or net losses of ecosystem carbon storage are negative. Markers show the average NM across the three case study sites, and error bars denote the range. Quantitative flow diagrams illustrate the average carbon fluxes in representative BECCS (*B*) and reforestation (*C*) scenarios. To reduce visual clutter in *B*, a small (1.5 Mg CO_2 ha^{-1} y^{-1}) BRE term is combined into the TP_{bfuel} term, BSC emissions (1.2 Mg CO_2 ha^{-1} y^{-1}, excluding N_2O) are subtracted out from the AFFE term, and the CCS term includes a small (0.5 Mg CO_2 ha^{-1} y^{-1}) component representing carbon sequestration as gasification char by-product applied to soils.

secondary forest conversion scenarios), which is within the range of previous model-based analyses (42). This value falls within our estimated range for reforestation on former agricultural land and is 250% greater than that of grassland restoration. In contrast, clearing secondary forest for switchgrass production results in a large up-front loss of ecosystem carbon storage (i.e., negative NECB) that is not offset by fossil fuel displacement via current-day cellulosic ethanol production (using both the harvested wood and subsequently cultivated switchgrass) over the first 30 y of the assessment.

Future BECCS systems offer improved performance through higher switchgrass and fuel yields and the direct geological sequestration of CO_2 in amounts greater than the reforestation carbon sink (*SI Appendix*, Table S1). Comparative carbon fluxes for the future BECCS and reforestation scenarios on abandoned cropland are illustrated in Fig. 4 *B* and *C*, respectively. *SI Appendix*, Fig. S4 presents mitigation results normalized by NPP to illustrate whether higher-performing scenarios are more effective at achieving mitigation per unit of carbon fixed, or whether they simply fix more carbon per hectare. Reforestation achieves 0.6 Mg of net ecosystem carbon storage for every 1 Mg of net primary production carbon (Mg NPP-C). The future BECCS scenario achieves a comparable NPP-normalized NM of 0.7 Mg C-equivalent (Ce) per 1 Mg NPP-C via a combination of ecosystem carbon storage, net fossil fuel displacement, and CCS. However, total NPP for future switchgrass production is on average approximately 3.5 times higher than that of unmanaged secondary forest regrowth. Together, this results in four times the total per-hectare NM for the future BECCS scenario as compared with reforestation. Similarly, the NPP-normalized NM of current-day switchgrass ethanol [0.2 Mg Ce (Mg NPP-C)$^{-1}$] is only about 20% higher than that of grassland restoration, but managed switchgrass production achieves approximately twice the NPP, resulting in 2.5 times more total mitigation than grassland restoration. Most starkly, the future BECCS scenario achieves approximately 5 times the NPP-normalized NM and 3 times the total NPP of grassland restoration, which combined result in ∼15 times the total mitigation potential compared with that scenario.

Indirect Emissions in Perspective

The analysis presented thus far has accounted for the direct GHG impacts of cellulosic BP or natural vegetation restoration/retention as illustrated in Fig. 2. These estimates likely capture the full GHG impact of those scenarios when deployed on retired or abandoned cropland (15) or in cases of "land sparing" via future agricultural intensification (17) or dietary shifts (18). Wider-scale deployment of biofuel and other land-based CDR technologies in competition with existing agriculture incurs risk of ILUC effects (14). External estimates of such ILUC emissions can theoretically be added to the direct GHG mitigation potential assessed here to estimate total net life cycle GHG impacts (43) in those cases. However, most recent economic assessment studies report only total "induced" LUC, a metric that aggregates together both ILUC and the direct changes in carbon storage in the fields where biofuel feedstock crops are grown (*SI Appendix*, Fig. S5). Sometimes, this total induced LUC is broken down into domestic and international components. In practice, it is often impossible to harmonize and downscale such estimates (which reflect economically optimal land use responses at very coarse spatial scales) to the more targeted land conversion scenarios of our assessment. It is nonetheless still illustrative to compare the magnitude of these prior literature estimates with the bioenergy system design factors assessed here.

Fig. 5 shows our modeling results alongside estimates of total induced LUC emissions for cellulosic BP from perennial grasses (switchgrass, Miscanthus, or unspecified) compiled from various prior analyses (44) and from the Argonne National Laboratory Carbon Calculator for Land Use Change from Biofuels Production (CCLUB) model (45), as summarized in *SI Appendix*, Table S2. The average biomass yield assumed across the studies that considered a switchgrass feedstock (13.1 Mg ha^{-1} y^{-1}) is within the range simulated for our present-day switchgrass biofuel scenarios. The average yield assumed across the studies that

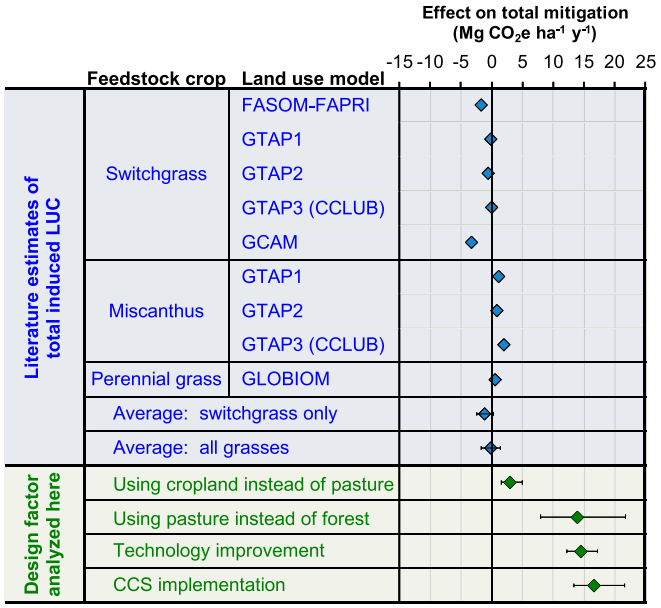

Fig. 5. Literature estimates of total induced LUC compared with the system design factors assessed here. LUC emissions estimates are adapted from those compiled in Pavlenko and Searle (44) and from the Argonne National Laboratory CCLUB model (45). Biofuel system design factors consist of targeted feedstock production on cropland and avoidance of secondary forest conversion, switchgrass yield and biofuel conversion technology improvements, and sequestration of the biorefinery CO_2 by-product via CCS. Land conversion choices are evaluated in terms of differences in total per-hectare NM from cropland, pasture, or secondary forest conversion to BP. Avoided emissions and carbon sequestration are positive mitigation; new fossil emissions or net losses of ecosystem carbon storage are negative. Error bars denote the full range of results across all relevant analysis scenarios and case study sites.

considered a Miscanthus feedstock (17.5 Mg ha^{-1} y^{-1}) is representative of current yields for that crop and consistent with our higher-yielding future switchgrass biofuel scenarios (*DayCent Modeling*). These studies considered cellulosic ethanol production at scales of 27 to 34 billion liters of ethanol annually, approximately half the amount of cellulosic biofuel mandated by the US Energy Independence and Security Act of 2007 (46). This scale is smaller than that called for in some climate stabilization scenarios (7), and such wider bioenergy deployment could lead to larger indirect emissions consequences.

Total induced LUC estimates range from a net emission of 3.3 Mg CO_2e ha^{-1} y^{-1} to a net sequestration of 1.9 Mg CO_2e ha^{-1} y^{-1}. The average for the switchgrass studies is a net emission of 1.13 Mg CO_2e ha^{-1} y^{-1}, and the average across all studies is a net emission of 0.13 Mg CO_2e ha^{-1} y^{-1}. While the highest total induced LUC estimates are of comparable magnitude with our estimates of the direct mitigation potential from grassland restoration, they are significantly smaller than our estimates of the direct mitigation potential from current-day cellulosic ethanol production. Our analysis suggests that cellulosic biofuel system GHG performance can be improved by 14 Mg CO_2e ha^{-1} y^{-1} by cultivating switchgrass feedstock on former pasture rather than converting secondary forest or by an additional 3 Mg CO_2e ha^{-1} y^{-1} by targeting cropland over pasture. Future switchgrass and biorefinery fuel yield improvements and CCS adoption can additionally improve the NM of biofuel systems by 15 and 17 Mg CO_2e ha^{-1} y^{-1}, respectively. The international share of total induced LUC estimates is broken out where possible in *SI Appendix*, Table S2. Our average estimates for the NM of current-day biofuel and future BECCS scenarios are 12 and 68 times greater, respectively, than the average of all international LUC emissions estimates and 3 and 18 times greater, respectively, than the highest estimate.

There are other potential indirect effects of biofuel deployment beyond ILUC. Geographically uneven adoption of GHG mitigation policies could cause biofuel use in one country to lower global petroleum prices, leading to higher petroleum consumption elsewhere (i.e., a rebound effect). The magnitude and sign of such an emissions effect from the deployment of first-generation food-based biofuels are disputed (47, 48) and depend heavily on the exact structure of biofuel support and the presence of other GHG mitigation policies (e.g., carbon taxes or emissions trading schemes) both domestically and globally. A large rebound effect could potentially offset much of the AFFE value of the conventional cellulosic biofuel systems assessed here (Fig. 4*A*). Rebound has only received a small fraction of the research attention that ILUC has and deserves further study, particularly since the question of whether renewable energy sources displace or supplement fossil fuel usage is not limited to biofuels (49). However, even in the absence of fossil fuel displacement benefits, we assess that future carbon-negative BECCS systems could still outperform reforestation based on their geological sequestration value alone (an effect not subject to such indirect market-based risks).

Discussion

Bioenergy assessment and policy development have often been limited by the simplifying but inaccurate assumption of biomass carbon neutrality (50, 51). In response, a variety of studies (26–28) have called for explicit accounting of ecosystem carbon fluxes as an alternative to the carbon neutrality assumption and for comparison with alternative land uses in order to better understand the true biophysical mitigation potential of bioenergy systems (19, 22, 23, 42, 52). Our analysis addresses both points, using well-calibrated models of ecosystem carbon fluxes and stocks to evaluate both bioenergy and alternate land use scenarios. We find the following.

BP from switchgrass cultivated on former agricultural lands avoids carbon debt, resulting in immediate net mitigation potential (Fig. 3). Conversion of secondary forest to BP results in ecosystem carbon debts requiring several years to several decades or more to overcome, depending on conversion technology and whether CCS is employed.

Current-day cellulosic BP on former agricultural land results in much greater mitigation potential than grassland restoration, similar to the carbon opportunity cost of reforestation at sites that would support forest (Figs. 3 and 4). Future technology improvement and CCS integration could further improve bioenergy system per-hectare mitigation potential by a factor of approximately six relative to current-day performance.

Several factors analyzed in this study—initial land cover, maturity of production technology, and CCS use—have much larger impacts on mitigation performance than recent literature estimates of both total induced LUC and international LUC effects associated with perennial grass feedstock cultivation (Fig. 5).

There is growing recognition that implementation of land-based biological mitigation strategies needs to be both rapid and robust. In this context, it should be noted that biomass production for bioenergy generates new revenue streams for landowners outside of payment schemes for carbon or other ecosystem services, which could help incentivize quicker or more widespread adoption of land-based biological mitigation. In addition, bioenergy systems configured for negative emissions via CCS (as assessed here) or biochar coproduction (8) are likely to achieve durable carbon sequestration with less vulnerability to

future changes in land use, disturbance regimes (e.g., wildfire, insect outbreaks), or local climate shifts that could reduce the mitigation value of restored grasslands or especially forests (53, 54). Our mitigation estimates for vegetation restoration are generous in that we did not explicitly simulate ecosystem sink saturation or potential disturbance [focusing on NECB instead of the more widely scoped "net biome production" metric (30)], or consider how periodic harvest in the secondary forest conversion scenarios could be managed spatially to maintain consistent carbon storage at landscape scales (55).

There are many other considerations in land management other than GHG mitigation, and landowners often have to navigate trade-offs between creating economic value and maintaining or enhancing biodiversity and ecosystem services (56). The rapid scale-up of any land-based mitigation or CDR scheme will challenge assessment practice and governance structures to ensure sustainable and desirable outcomes (57). However, greater consideration of land management for climate change mitigation will almost certainly be necessary to achieve climate stabilization goals, with or without bioenergy (2, 3). That is likely best achieved through development of a portfolio of multiple land-based biological mitigation options (1), and the most useful corresponding assessments are those that can support decision making and optimization among the competing options in different locations and contexts. In addition to the biophysical potential for GHG mitigation as assessed here, decision criteria should include factors outside the scope of this analysis, such as costs, wildlife and biodiversity impacts or benefits, other ecosystem services, and sustainable development and social equity outcomes.

Our results—particularly those for future biofuel technology scenarios—stand in sharp contrast to recent critiques that advocate eliminating policy support for bioenergy technology research (25) and deployment (24). We note that continued research, development, and iterative limited-scale deployment of such systems are essential for realizing improvements and cost reductions in biorefining and CCS technology (58, 59) in support of existing renewable fuel mandates and in time for the mid-century wide-scale deployment of CDR called for in many projections. Furthermore, real-world empirical data on energy crop adoption and performance (37, 60) inform assessment science and provide guidance for ongoing bioenergy policy development. Net GHG mitigation is not an automatic outcome of any bioenergy system, and previous studies have illustrated a number of sustainability pitfalls that can erode system GHG benefits. However, these pitfalls are avoidable if policy makers and the bioenergy industry are mindful of them and design land use policies and bioenergy systems with intent accordingly. In particular, we show that cellulosic biofuels can be deployed today without significant carbon debt and achieve greater mitigation potential than restoration of natural vegetation in the case of grasslands. Moreover, the mitigation potential of projected future biofuel technology is severalfold higher. Across a wide range of land use and natural vegetation types, sustainable bioenergy systems can make an important and distinctive contribution to the climate stabilization challenge.

Materials and Methods

Carbon and Mitigation Accounting. *NECB* (30, 61) can be expressed in terms of changes in above- and belowground carbon stocks (ΔC_{AG} and ΔC_{BG}, respectively) or alternately, in terms of *NPP*, R_h, and *Harv* as follows (detailed derivation is available in *SI Appendix*):

$$NECB = \Delta C_{AG} + \Delta C_{BG} = NPP - R_h - Harv. \quad [1]$$

The net cumulative direct carbon-equivalent GHG exchange with the atmosphere (ΔC_{atm}) associated with a marginal increase in biofuel or bioenergy production (*bfuel*, as illustrated in Fig. 2) over a given assessment period is

$$\Delta C_{atm,\ bfuel} = BSC + BRE + TP_{bfuel} + R_{h,bfuel} - NPP_{bfuel}, \quad [2]$$

which includes *BSC* life cycle emissions associated with material inputs and energy use during switchgrass cultivation, harvest, and transport, as well as soil N_2O emissions; *BRE* of the biogenic CO_2 by-product of conversion; tailpipe emissions of biogenic carbon from biofuel combustion (TP_{bfuel}); and ecosystem carbon exchanges with the atmosphere, specifically NPP_{bfuel} and $R_{h,bfuel}$. Combining Eqs. **1** and **2**, this net atmospheric exchange can alternately be expressed in terms of changes in above- and belowground ecosystem carbon storage ($\Delta C_{AG,bfuel}$ and $\Delta C_{BG,bfuel}$, respectively) and biomass harvest:

$$\Delta C_{atm,\ bfuel} = BSC + BRE + TP_{bfuel} - (\Delta C_{AG,bfuel} + \Delta C_{BG,bfuel}) - Harv. \quad [3]$$

Assuming negligible supply chain biomass losses, a biorefinery carbon balance implies that a fraction of *Harv* carbon will be converted to biofuel and reemitted from vehicle tailpipes, and the remainder will be either emitted at the biorefinery (*BRE*) or geologically sequestered via *CCS*:

$$Harv = BRE + CCS + TP_{bfuel}. \quad [4]$$

Combining Eqs. **3** and **4**, the effect of the biofuel scenario on the atmosphere can be expressed more simply as new *BSC* emissions minus net ecosystem sequestration and geological carbon sequestration:

$$\Delta C_{atm,\ bfuel} = BSC - (\Delta C_{AG,bfuel} + \Delta C_{BG,bfuel}) - CCS. \quad [5]$$

The net cumulative direct exchange with the atmosphere in an alternative natural vegetation restoration scenario (*veg*) can be expressed similarly. However, the *veg* scenarios lack biomass harvest but include baseline conventional GSC and tailpipe emissions (*GSC* and TP_{veg}, respectively) in energy-equivalent amounts equal to BP in the biofuel scenario (assuming that BP offsets gasoline use on a 1:1 energy basis, ignoring any rebound effect):

$$\Delta C_{atm,\ veg} = GSC + TP_{veg} - (\Delta C_{AG,veg} + \Delta C_{BG,veg}). \quad [6]$$

Land-based biological mitigation is the purposeful management of land and photosynthetically derived carbon to reduce the net accumulation of CO_2 and other GHGs in the atmosphere via the displacement of fossil energy emissions and/or the direct sequestration of carbon. We thus calculate the net biophysical mitigation potential (*NM*) of a scenario as the opposite of the net cumulative direct carbon exchange with the atmosphere minus fluxes associated with baseline fossil fuel usage (*GSC* and TP_{veg}). For the *veg* scenarios, we build on Eq. **6** to calculate

$$\begin{aligned} NM_{veg} &= -(\Delta C_{atm,\ veg} - (GSC + TP_{veg})) \\ &= -((GSC + TP_{veg} - (\Delta C_{AG,veg} + \Delta C_{BG,veg})) - (GSC + TP_{veg})) \\ &= \Delta C_{AG,veg} + \Delta C_{BG,veg}. \end{aligned} \quad [7]$$

Since there is no displacement of conventional gasoline use in this scenario, land-based biological mitigation consists only of the net cumulative amount of carbon sequestered in above- and belowground ecosystem carbon pools over the assessment period. The equivalent for the biofuel scenarios is

$$\begin{aligned} NM_{bfuel} &= -(\Delta C_{atm,\ bfuel} - (GSC + TP_{veg})) \\ &= -((BSC - (\Delta C_{AG,bfuel} + \Delta C_{BG,bfuel}) - CCS) - (GSC + TP_{veg})) \\ &= -BSC + \Delta C_{AG,bfuel} + \Delta C_{BG,bfuel} + CCS + GSC + TP_{veg}. \end{aligned} \quad [8]$$

For simplicity, we define gross *AFFE* as the *GSC* and TP_{veg} emissions displaced by biofuel use:

$$AFFE = GSC + TP_{veg}. \quad [9]$$

Combining Eqs. **8** and **9**, we can express *NM* for the biofuel scenarios as the sum ecosystem carbon sequestration (or losses), geological carbon sequestration via *CCS*, and *AFFE* minus *BSC* emissions:

$$NM_{bfuel} = \Delta C_{AG,bfuel} + \Delta C_{BG,bfuel} + CCS + AFFE - BSC. \quad [10]$$

Eqs. **8** and **10** are the basis for the GHG mitigation values reported in the text and in Figs. 3 and 4.

DayCent Modeling. DayCent is a process-based ecosystem carbon, nitrogen, and water cycling model that simulates plant NPP, carbon partitioning, soil organic matter dynamics, and trace gas emissions on a daily time step (62). We used DayCent to estimate cellulosic biomass yields, changes in ecosystem carbon storage, and soil N_2O emissions (driven by synthetic nitrogen fertilizer application and other processes) for the various scenarios assessed. Our

analysis focused on cropland and pasture transitioning out of agriculture and into either switchgrass cultivation or restoration of natural forest or grassland (a reforestation terminology note is in *SI Appendix*), as shown schematically in *SI Appendix*, Fig. S2. Additional scenarios representing clear cutting of secondary forest and conversion to switchgrass vs. continued forest growth were also included for illustrative comparison with previous studies [e.g., Walker et al. (20)].

Case study counties were selected as having significant amounts of both pasture land and row cropping as per informal visual inspection of the Cropland Data Layer (63); having climate conditions suitable for cropland, grassland, or forest vegetation; and for having soils of diverse texture and ample depth as per the Soil Survey Geographic database (SSURGO) (64). Standard DayCent data inputs for soil texture and depth were derived from the SSURGO database, and weather inputs were from the North American Regional Reanalysis database (65), as described previously in Field et al. (34). Within each case study, the correlation between land quality and land use was represented by selecting a fine-textured soil (silt loam or similar) from among those present in the county to use for all simulations with a cropland initial condition, while a coarse-textured soil (sandy loam or similar) was used for simulations with pasture or forest initial condition, consistent with prior landscape-scale analysis (37).

Initialization of soil carbon and nitrogen levels was performed via simulation of presettlement land cover and historic land use consistent with the annual inventory of US GHG emissions and sinks conducted by the United States Environmental Protection Agency (EPA) (66). The resulting model initializations were then extended with 70-y forward simulations of biofuel feedstock production and ecosystem restoration scenarios as per *SI Appendix*, Fig. S2. Additional details on postprocessing DayCent simulation results to extract key ecosystem data (biomass harvest, changes in ecosystem carbon storage, NPP, R_h, and N_2O emissions) are available in *SI Appendix*. Accurate forward simulation requires both calibration of vegetation characteristics [tissue C:N ratio limits, temperature and moisture stress response, turnover of aboveground biomass and fine roots, and overall productivity potential (34)] and specification of realistic management.

Our current switchgrass simulations considered the lowland ecotype at the Louisiana case study site and upland switchgrass in Iowa and New York based on the parameterization and simple model of switchgrass phenology as a function of latitude described in Field et al. (34). We assumed annual fertilizer application at a rate of 50 kg N ha^{-1}, annual biomass harvest (excluding the planting year), and field tilling and replanting every 10 y. We adjusted switchgrass productivity down 15% to reflect deviations associated with scaling up field trial results to commercial scales (67). For the future switchgrass variety, we increased the potential productivity parameter in order to achieve a 64% higher average annual biomass yield, equivalent to a 2% annual yield increase compounded over 25 y. This higher-productivity variety was implemented at the beginning and held constant across the duration of the 70-y forward simulation. We note that maize yields in the United States initially increased at an annual rate of 3.5 to 6% with the advent of concerted breeding and management improvement efforts in the 1930s and were still increasing at an average rate of ∼1.5%/y in the 1990s (68). Our simulated future mean switchgrass yield of 18.4 Mg ha^{-1} y^{-1} is within the range of current-day yields achievable across most of the eastern United States with Miscanthus, energy cane, and sorghum cultivated in their most appropriate respective environments (38).

We conservatively modeled our grassland restoration scenarios using the current-day switchgrass parameterization, but without nitrogen fertilizer application or harvest, and subject to light seasonal grazing. We created regionally specific parameterizations of native forest growth based on the forest yield tables in Smith et al. (35) for the New York ["Northeast" region in Smith et al. (35)], Iowa ("Northern Prairie States"), and Louisiana ("South Central") case study sites, adjusting symbiotic nitrogen fixation for broad consistency with soil total nitrogen trend data from two representative afforestation studies (69, 70). Additional details on forest parameter calibration are available in *SI Appendix*.

Biorefinery and CCS Technology. Our current cellulosic BP scenario was modeled on the "base" biochemical conversion pathway of dilute acid pretreatment and simultaneous saccharification and fermentation to ethanol described in Laser et al. (40). This pathway is broadly consistent with the six pioneer commercial-scale cellulosic biorefineries that had been constructed worldwide as of 2017, with a combined nameplate annual production capacity of 450 million L (58). Ethanol yield is estimated at 318 L per dry metric ton of biomass feedstock, equivalent to 40.4% of the energy content of the feedstock biomass (evaluated on a lower heating value [LHV] basis). Recovered fermentation residues are combusted to power a Rankine cycle for generation of biorefinery process steam and electricity needs, with a net electricity export of 11.5 megawatts (MW; 2.9% of feedstock LHV).

Cellulosic ethanol production has only become a commercial reality during the last few years, and both experience-driven cost reductions within current processing paradigms as well as alternative processing paradigms with potential for large cost reductions and yield improvements are anticipated (71). We also considered a future hybrid biochemical–thermochemical conversion case (72) based on ammonia fiber expansion pretreatment and consolidated bioprocessing to ethanol, followed by gasification of fermentation resides and single-pass FT conversion of the resulting syngas to gasoline- and diesel-weight FT liquids (41). This future case yields 54.1% of feedstock LHV as ethanol [440 L (Mg biomass)$^{-1}$], 9.7% as FT diesel, and 6.1% as FT gasoline. The residual syngas not converted to FT liquids is combusted to produce biorefinery steam and electricity needs in a gas turbine combined cycle power island, with 5 MW (1.3%) net electricity export. Note that, in addition to the future increase in switchgrass yields discussed previously, the future conversion technology design assumes concurrent improvements in feedstock quality, specifically a 10% increase in carbohydrate content and 50% reduction in ash (40). The gasification process also produces a small amount of char, which we assume is soil applied with 80% long-term carbon retention (73).

The future biorefinery design features a number of by-product streams of high-purity CO_2 that are amenable to CCS. We used data from a coal- and biomass-to-liquids CCS study with similar fuel yield assumptions [Liu et al. (74)] to estimate CO_2 recovery rates and associated CCS parasitic energy requirements. The initial fermentation step in our future biorefinery produces CO_2 at a 1:1 stoichiometric ratio with ethanol, corresponding to 17.9% of input biomass carbon. Associated parasitic electricity requirement for gas dehydration, compression, and injection of that carbon dioxide was estimated at 27 MJ_e (Mg CO_2)$^{-1}$. During the subsequent thermochemical processing of fermentation residues, a syngas cleanup step improves once-through FT reactor yields while creating an additional by-product stream of CO_2. Liu et al. (74) also considered autothermal reforming, water–gas shift, and CO_2 removal from the unconverted syngas downstream of the FT reactor prior to combustion. Together, these two additional CO_2 streams comprise 30.2% of input biomass carbon, and we estimated an associated CCS parasitic energy requirement of 75 MJ_e (Mg CO_2)$^{-1}$ for the additional separation, dehydration, compression, and injection steps. Full biorefinery carbon balances are detailed in *SI Appendix*, Table S1.

Supply Chain Emissions and Displacement Factors. Life cycle emissions associated with farm inputs, on-farm energy use, farm–biorefinery transport, and biorefinery inputs were estimated using the Argonne National Laboratory Greenhouse Gases, Regulated Emissions, and Energy Use in Transportation (GREET) life cycle assessment model (75), specifically GREET 2018 database version 13395. GREET evaluates the life cycle 100-y global warming potential from CO_2 and other GHGs (e.g., methane and N_2O) and climate forcing agents (e.g., black carbon) for different transportation technologies and their associated technosphere inputs. Farm inputs and energy use rates were modified within the "switchgrass production for ethanol plant" pathway based on a previously published model of switchgrass cultivation (37). That model includes per-area estimates of farm operation diesel fuel use and nutrient, herbicide, and lime application, as well as estimates of harvest operation fuel use and nutrient replacement requirements on a per-ton biomass-harvested basis. We retained the GREET default assumption for switchgrass farm–biorefinery transport of 106 km (one way) via heavy-duty truck. The field-to-biorefinery gate footprint associated with these inputs and energy use was then evaluated in GREET over a range of switchgrass per-area yield assumptions, enabling us to fit a simple model (power regression) of that footprint as a continuous function of yield, which could be integrated into our python code and applied to our DayCent-derived yield estimates (*SI Appendix*, Fig. S6). For simplicity, the same life cycle emissions footprint model was also applied to wood harvested in scenarios of secondary forest conversion to switchgrass, and we assumed that feedstock would also be processed via the same biorefinery process described in the previous section.

Most biorefinery process energy and electricity requirements are met through combustion of conversion by-products. However, other biorefinery inputs include sulfuric acid and/or ammonia for biomass pretreatment, lime for process pH control, corn steep liquor for fermentation organism nutrients, and water to make up losses from wastewater treatment and elsewhere in the system. These inputs were estimated from Laser et al. (40), tables 12 and 13 subject to a 0.5% mass cutoff rule (excluding makeup water mass from that total) and used to adjust the default GREET "coproduction of ethanol and power from switchgrass" pathway. Liquid biofuels and

electricity produced by our simulated biorefinery were assumed to displace conventional gasoline, diesel, and US mix grid electricity on a 1:1 energy basis (in Fig. 2, note that electricity coproduction is omitted for simplicity). The well-to-wheel life cycle emissions footprint of each megajoule of conventional fuel (including both tailpipe emissions and upstream emissions associated with petroleum extraction and refining) or grid electricity displaced was estimated using emissions factors extracted from GREET, evaluated in the year 2019 for the current bioenergy scenario and in 2044 for the future scenario. Note that the biorefineries in both of those scenarios are net electricity exporters, although the addition of CCS in the future scenario tips the biorefinery over to a small electricity importer (*SI Appendix*, Table S1).

Literature Estimates of Total Induced LUC. Pavlenko and Searle (44) compiled a survey of prior literature total induced LUC estimates for switchgrass, Miscanthus, and unspecified perennial energy grasses made using a variety of global agricultural trade models. The EPA used the Forest and Agricultural Sector Optimization Model combined with the Food and Agricultural Policy Research Institute model (FASOM-FAPRI) to estimate LUC emissions associated with 30 GL of annual cellulosic ethanol production from switchgrass feedstocks, as detailed in their regulatory impact analysis for the US renewable fuel standard (76). Plevin and Mishra (77) conducted a similar analysis using the Global Change Assessment Model (GCAM) considering 34 GL y^{-1} of switchgrass ethanol production. The Global Trade Analysis Project (GTAP) model has been used to predict the land use response to 27 GL y^{-1} of ethanol production from either switchgrass or Miscanthus feedstocks (78). Multiple teams have subsequently applied different ecosystem carbon stock estimates to those results in order to estimate LUC emissions (45, 79, 80). Finally, Valin et al. (81) used the Global Biosphere Management Model (GLOBIOM) to consider the LUC impacts of cellulosic ethanol production from perennial grass cultivation in Europe.

Together, these comprise nine estimates of total induced LUC impacts for the large-scale production of cellulosic ethanol from dedicated perennial energy grasses, assessed using four different economic models. Those LUC modeling results are detailed in *SI Appendix*, Table S2 using the sign convention that positive values denote net emissions to atmosphere and negative denotes net sequestration. LUC estimates are typically reported on a fuel basis in units of grams of carbon dioxide equivalent emissions per megajoule of fuel produced (g CO_2e MJ^{-1}). In order to convert these estimates to a per-area basis for comparison with the rest of our analysis, we used the total BP rate, energy crop yield, and total direct land use values assumed or predicted in each study [as compiled by Pavlenko and Searle (44)] to back calculate the ethanol yield per ton of cellulosic biomass, and then we expressed the per-megajoule total induced LUC results on a per-hectare basis in units of megagrams of carbon dioxide equivalent emissions per hectare per year (Mg CO_2e ha^{-1} y^{-1}) instead. Insufficient information was reported for the GLOBIOM model to back calculate the fuel yield per megagram of biomass, so we used the average value across the other studies in that case.

The international LUC component of total induced LUC was broken out for six of the nine sets of LUC results examined (44, 45). We converted those results from a per-megajoule to a per-hectare basis in the same manner as above. These data provide an alternate point of comparison for our direct mitigation estimates since they isolate international market-mediated agricultural extensification and intensification effects (which we did not assess in our modeling), excluding the confounding (and often compensatory) effect of direct soil carbon sequestration on the land where those crops are cultivated (which is already included in our assessment).

Data Availability. All data, code, and models underlying this analysis are available in an online open access repository, Figshare (https://doi.org/10.6084/m9.figshare.5760768). DayCent model calibration, initialization, scenario simulation, and results analysis were automated in Python 2.7. A UNIX executable version of the DayCent model (https://www2.nrel.colostate.edu/projects/daycent/) is included in the Figshare repository.

ACKNOWLEDGMENTS. We thank Dennis Ojima and Daniel L. Sanchez for their encouragement on this topic. We acknowledge partial support as follows: São Paulo Research Foundation (FAPESP) Grant 2014/26767-9 (to J.L.F., T.L.R., E.A.H.S., J.J.S., and L.R.L.); The Center for Bioenergy Innovation (CBI), a US Department of Energy (DOE) Research Center supported by Office of Biological and Environmental Research in the DOE Office of Science under Grant DE-AC05-00OR22725 (to J.L.F., T.L.R., K.P., and L.R.L.); US Department of Agriculture National Institute of Food and Agriculture (USDA/NIFA) Grants 2013-68005-21298 (to J.L.F. and K.P.), 2017-67019-26327 (to J.L.F. and K.P.), and 2012-68005-19703 (to T.L.R.); The Center for Advanced Bioenergy and Bioproducts Innovation (CABBI), a DOE Research Center supported by Office of Biological and Environmental Research in the DOE Office of Science under Grant DE-AC05-SC0018420 (to D.S.L. and S.P.L.); the Energy Biosciences Institute (D.S.L. and S.P.L.); the São Paulo Research Foundation (L.R.L.); and the Link Foundation (L.R.L.).

1. J. G. Canadell, E. D. Schulze, Global potential of biospheric carbon management for climate mitigation. *Nat. Commun.* **5**, 5282 (2014).
2. D. P. van Vuuren *et al*., Alternative pathways to the 1.5 °C target reduce the need for negative emission technologies. *Nat. Clim. Chang.* **8**, 391–397 (2018).
3. J. Rogelj *et al*, Mitigation pathways compatible with 1.5 °C in the context of sustainable development. https://www.ipcc.ch/site/assets/uploads/sites/2/2019/02/SR15_Chapter2_Low_Res.pdf. Accessed 10 August 2020.
4. L. M. Fulton, L. R. Lynd, A. Körner, N. Greene, L. R. Tonachel, The need for biofuels as part of a low carbon energy future. *Biofuels Bioprod. Biorefin.* **9**, 476–483 (2015).
5. S. J. Davis *et al*., Net-zero emissions energy systems. *Science* **360**, eaas9793 (2018).
6. D. Tilman, J. Hill, C. Lehman, Carbon-negative biofuels from low-input high-diversity grassland biomass. *Science* **314**, 1598–1600 (2006).
7. S. Fuss *et al*., Betting on negative emissions. *Nat. Clim. Chang.* **4**, 850–853 (2014).
8. J. Lehmann, A handful of carbon. *Nature* **447**, 143–144 (2007).
9. D. L. Sanchez, N. Johnson, S. T. McCoy, P. A. Turner, K. J. Mach, Near-term deployment of carbon capture and sequestration from biorefineries in the United States. *Proc. Natl. Acad. Sci. U.S.A.* **115**, 4875–4880 (2018).
10. P. A. Turner, C. B. Field, D. B. Lobell, D. L. Sanchez, K. J. Mach, Unprecedented rates of land-use transformation in modelled climate change mitigation pathways. *Nat. Sustain.* **1**, 240–245 (2018).
11. T. L. Richard, Challenges in scaling up biofuels infrastructure. *Science* **329**, 793–796 (2010).
12. A. E. Farrell *et al*., Ethanol can contribute to energy and environmental goals. *Science* **311**, 506–508 (2006).
13. J. Fargione, J. Hill, D. Tilman, S. Polasky, P. Hawthorne, Land clearing and the biofuel carbon debt. *Science* **319**, 1235–1238 (2008).
14. T. Searchinger *et al*., Use of U.S. croplands for biofuels increases greenhouse gases through emissions from land-use change. *Science* **319**, 1238–1240 (2008).
15. A. Zumkehr, J. E. Campbell, U. S. Historical, Historical U.S. cropland areas and the potential for bioenergy production on abandoned croplands. *Environ. Sci. Technol.* **47**, 3840–3847 (2013).
16. I. Gelfand *et al*., Sustainable bioenergy production from marginal lands in the US Midwest. *Nature* **493**, 514–517 (2013).
17. A. Lamb *et al*., The potential for land sparing to offset greenhouse gas emissions from agriculture. *Nat. Clim. Chang.* **6**, 488–492 (2016).
18. D. Tilman, M. Clark, Global diets link environmental sustainability and human health. *Nature* **515**, 518–522 (2014).
19. R. Righelato, D. V. Spracklen, Environment. Carbon mitigation by biofuels or by saving and restoring forests? *Science* **317**, 902 (2007).
20. T. Walker *et al*., Biomass sustainability and carbon policy study. *Manomet Center for Conservation Sciences* (2010). https://www.manomet.org/wp-content/uploads/2018/03/Manomet_Biomass_Report_Full_June2010.pdf. Accessed 10 August 2019.
21. J. F. Beckman, S. Evans, R. D. Sands, "U.S. renewable fuel standard 2: Impacts of cellulosic biofuel production" in Agricultural and Applied Economics Association 2011 AAEA & NAREA Joint Annual Meeting. https://ageconsearch.umn.edu/record/103751/. Accessed 7 March 2020.
22. H. Haberl, Net land-atmosphere flows of biogenic carbon related to bioenergy: Towards an understanding of systemic feedbacks. *Global Change Biol. Bioenergy* **5**, 351–357 (2013).
23. S. L. Lewis, C. E. Wheeler, E. T. A. Mitchard, A. Koch, Restoring natural forests is the best way to remove atmospheric carbon. *Nature* **568**, 25–28 (2019).
24. T. D. Searchinger, T. Beringer, A. Strong, Does the world have low-carbon bioenergy potential from the dedicated use of land? *Energy Policy* **110**, 434–446 (2017).
25. J. M. DeCicco, W. H. Schlesinger, Opinion: Reconsidering bioenergy given the urgency of climate protection. *Proc. Natl. Acad. Sci. U.S.A.* **115**, 9642–9645 (2018).
26. J. M. DeCicco, Biofuel's carbon balance: Doubts, certainties and implications. *Clim. Change* **121**, 801–814 (2013).
27. J. M. DeCicco *et al*., Carbon balance effects of U.S. biofuel production and use. *Clim. Change* **138**, 667–680 (2016).
28. T. Searchinger, Biofuels and the need for additional carbon. *Environ. Res. Lett.* **5**, 024007 (2010).
29. H. Haberl *et al*., Correcting a fundamental error in greenhouse gas accounting related to bioenergy. *Energy Policy* **45**, 18–23 (2012).
30. F. S. Chapin *et al*., Reconciling carbon-cycle concepts, terminology, and methods. *Ecosystems* **9**, 1041–1050 (2006).
31. M. Abraha, I. Gelfand, S. K. Hamilton, J. Chen, G. P. Robertson, Carbon debt of field-scale conservation reserve program grasslands converted to annual and perennial bioenergy crops. *Environ. Res. Lett.* **14**, 024019 (2019).
32. T. Zenone, I. Gelfand, J. Chen, S. K. Hamilton, G. P. Robertson, From set-aside grassland to annual and perennial cellulosic biofuel crops: Effects of land use change on carbon balance. *Agric. For. Meteorol.* **182–183**, 1–12 (2013).

33. S. J. Del Grosso, W. J. Parton, C. A. Keough, M. Reyes-Fox, "Special features of the DayCent modeling package and additional procedures for parameterization, calibration, validation, and applications" in *Advances in Agricultural Systems Modeling*, L. R. Ahuja, L. Ma, Eds. (Methods of Introducing System Models into Agricultural Research, American Society of Agronomy, Crop Science Society of America, Soil Science Society of America, 2011), pp. 155–176.
34. J. L. Field, E. Marx, M. Easter, P. R. Adler, K. Paustian, Ecosystem model parameterization and adaptation for sustainable cellulosic biofuel landscape design. *Global Change Biol. Bioenergy* **8**, 1106–1123 (2016).
35. J. E. Smith, L. S. Heath, K. E. Skog, R. A. Birdsey, Methods for calculating forest ecosystem and harvested carbon with standard estimates for forest types of the United States (2006). https://www.treesearch.fs.fed.us/pubs/22954. Accessed 22 November 2016.
36. C. C. Brandt, *et al*., "2016 Billion-ton report: Advancing domestic resources for a thriving bioeconomy, Volume 1: Economic availability of feedstocks" (Tech. Rep. ORNL/TM-2016/160, Oak Ridge National Laboratory, Oak Ridge, TN, 2016).
37. J. L. Field *et al*., High-resolution techno–ecological modelling of a bioenergy landscape to identify climate mitigation opportunities in cellulosic ethanol production. *Nat. Energy* **3**, 211–219 (2018).
38. D. K. Lee *et al*., Biomass production of herbaceous energy crops in the United States: Field trial results and yield potential maps from the multiyear regional feedstock partnership. *Global Change Biol. Bioenergy* **10**, 698–716 (2018).
39. D. Baldocchi, J. Penuelas, The physics and ecology of mining carbon dioxide from the atmosphere by ecosystems. *Global Change Biol.* **25**, 1191–1197 (2019).
40. M. Laser, H. Jin, K. Jayawardhana, L. R. Lynd, Coproduction of ethanol and power from switchgrass. *Biofuels Bioprod. Biorefin.* **3**, 195–218 (2009).
41. M. Laser, H. Jin, K. Jayawardhana, B. E. Dale, L. R. Lynd, Projected mature technology scenarios for conversion of cellulosic biomass to ethanol with coproduction thermochemical fuels, power, and/or animal feed protein. *Biofuels Bioprod. Biorefin.* **3**, 231–246 (2009).
42. S. G. Evans, B. S. Ramage, T. L. DiRocco, M. D. Potts, Greenhouse gas mitigation on marginal land: A quantitative review of the relative benefits of forest recovery versus biofuel production. *Environ. Sci. Technol.* **49**, 2503–2511 (2015).
43. US Environmental Protection Agency, Framework for assessing biogenic CO2 emissions from stationary sources (2014). https://yosemite.epa.gov/sab/sabproduct.nsf/0/3235DAC747C16FE985257DA90053F252/$File/Framework-for-Assessing-Biogenic-CO2-Emissions+(Nov+2014).pdf. Accessed 10 August 2019.
44. N. Pavlenko, S. Searle, "White paper on a comparison of induced land-use change emissions estimates from energy crops" (The International Council on Clean Transportation, 2018; https://theicct.org/publications/comparison-ILUC-emissions-estimates-energy-crops).
45. Z. Qin, J. B. Dunn, H. Kwon, S. Mueller, M. M. Wander, Influence of spatially dependent, modeled soil carbon emission factors on life-cycle greenhouse gas emissions of corn and cellulosic ethanol. *Global Change Biol. Bioenergy* **8**, 1136–1149 (2016).
46. 110th Congress of the United States, Energy Independence and Security Act of 2007 (2007). https://www.congress.gov/bill/110th-congress/house-bill/6/text. Accessed 30 September 2010.
47. D. Rajagopal, G. Hochman, D. Zilberman, Indirect fuel use change (IFUC) and the lifecycle environmental impact of biofuel policies. *Energy Policy* **39**, 228–233 (2011).
48. E. Smeets *et al*., The impact of the rebound effect of the use of first generation biofuels in the EU on greenhouse gas emissions: A critical review. *Renew. Sustain. Energy Rev.* **38**, 393–403 (2014).
49. R. York, Do alternative energy sources displace fossil fuels? *Nat. Clim. Chang.* **2**, 441–443 (2012).
50. M. Norton *et al*., Serious mismatches continue between science and policy in forest bioenergy. *Global Change Biol. Bioenergy* **11**, 1256–1263 (2019).
51. W. H. Schlesinger, Are wood pellets a green fuel? *Science* **359**, 1328–1329 (2018).
52. A. B. Harper *et al*., Land-use emissions play a critical role in land-based mitigation for Paris climate targets. *Nat. Commun.* **9**, 2938 (2018).
53. P. Dass, B. Z. Houlton, Y. Wang, D. Warlind, Grasslands may be more reliable carbon sinks than forests in California. *Environ. Res. Lett.* **13**, 074027 (2018).
54. J. F. Bastin *et al*., The global tree restoration potential. *Science* **365**, 76–79 (2019).
55. O. Cintas *et al*., The potential role of forest management in Swedish scenarios towards climate neutrality by mid century. *For. Ecol. Manage.* **383**, 73–84 (2017).
56. G. P. Robertson *et al*., Cellulosic biofuel contributions to a sustainable energy future: Choices and outcomes. *Science* **356**, eaal2324 (2017).
57. C. Robledo-Abad *et al*., Bioenergy production and sustainable development: Science base for policymaking remains limited. *Global Change Biol. Bioenergy* **9**, 541–556 (2017).
58. L. R. Lynd *et al*., Cellulosic ethanol: Status and innovation. *Curr. Opin. Biotechnol.* **45**, 202–211 (2017).
59. D. M. Reiner, Learning through a portfolio of carbon capture and storage demonstration projects. *Nat. Energy* **1**, 15011 (2016).
60. C. K. Wright, B. Larson, T. J. Lark, H. K. Gibbs, Recent grassland losses are concentrated around U.S. ethanol refineries. *Environ. Res. Lett.* **12**, 044001 (2017).
61. G. M. Lovett, J. J. Cole, M. L. Pace, Is net ecosystem production equal to ecosystem carbon accumulation? *Ecosystems* **9**, 152–155 (2006).
62. W. J. Parton, M. Hartman, D. Ojima, D. Schimel, DAYCENT and its land surface submodel: Description and testing. *Global Planet. Change* **19**, 35–48 (1998).
63. C. Boryan, Z. Yang, R. Mueller, M. Craig, Monitoring US agriculture: The US Department of Agriculture, National Agricultural Statistics Service, cropland data layer program. *Geocarto Int.* **26**, 341–358 (2011).
64. D. J. Ernstrom, D. Lytle, Enhanced soils information systems from advances in computer technology. *Geoderma* **60**, 327–341 (1993).
65. F. Mesinger *et al*., North American regional reanalysis. *Bull. Am. Meteorol. Soc.* **87**, 343–360 (2006).
66. US Environmental Protection Agency, Inventory of U.S. greenhouse gas emissions and sinks: 1990-2018 (2020). https://www.epa.gov/ghgemissions/inventory-us-greenhouse-gas-emissions-and-sinks-1990-2018. Accessed 18 May 2020.
67. S. Y. Searle, C. J. Malins, Will energy crop yields meet expectations? *Biomass Bioenergy* **65**, 3–12 (2014).
68. S. B. McLaughlin, J. R. Kiniry, C. M. Taliaferro, D. De La Torre Ugarte, "Projecting yield and utilization potential of switchgrass as an energy crop" in *Advances in Agronomy*, (Academic Press, Cambridge, MA, 2006), Vol. 90, pp. 267–297.
69. J. M. H. Knops, D. Tilman, Dynamics of soil nitrogen and carbon accumulation for 61 years after agricultural abandonment. *Ecology* **81**, 88–98 (2000).
70. E. A. Paul, S. J. Morris, J. Six, K. Paustian, E. G. Gregorich, Interpretation of soil carbon and nitrogen dynamics in agricultural and afforested soils. *Soil Sci. Soc. Am. J.* **67**, 1620–1628 (2003).
71. L. R. Lynd, The grand challenge of cellulosic biofuels. *Nat. Biotechnol.* **35**, 912–915 (2017).
72. M. Laser *et al*., Comparative analysis of efficiency, environmental impact, and process economics for mature biomass refining scenarios. *Biofuels Bioprod. Biorefin.* **3**, 247–270 (2009).
73. K. G. Roberts, B. A. Gloy, S. Joseph, N. R. Scott, J. Lehmann, Life cycle assessment of biochar systems: Estimating the energetic, economic, and climate change potential. *Environ. Sci. Technol.* **44**, 827–833 (2010).
74. G. Liu, E. D. Larson, R. H. Williams, T. G. Kreutz, X. Guo, Making Fischer–Tropsch fuels and electricity from coal and biomass: Performance and cost analysis. *Energy Fuels* **25**, 415–437 (2011).
75. M. Wang, M. Wu, H. Huo, Life-cycle energy and greenhouse gas emission impacts of different corn ethanol plant types. *Environ. Res. Lett.* **2**, 024001 (2007).
76. US Environmental Protection Agency, Assessment and Standards Division, Office of Transportation and Air Quality, Renewable fuel standard program (RFS2) regulatory impact analysis (2010). https://nepis.epa.gov/Exe/ZyPURL.cgi?Dockey=P1006DXP.TXT. Accessed 11 March 2019.
77. R. Plevin, G. Mishra, Estimates of the land-use-change carbon intensity of ethanol from switchgrass and corn stover using the GCAM 4.0 model. Report to Environmental Working Group (2015). http://static.ewg.org/reports/2015/better-biofuels-ahead/plevinreport.pdf. Accessed 11 March 2019.
78. F. Taheripour, W. E. Tyner, M. Q. Wang, Global land use changes due to the US cellulosic biofuel program simulated with the GTAP model. Argonne National Laboratory (2011). https://greet.es.anl.gov/publication-luc_ethanol. Accessed 11 March 2019.
79. J. B. Dunn, S. Mueller, H. Y. Kwon, M. Q. Wang, Land-use change and greenhouse gas emissions from corn and cellulosic ethanol. *Biotechnol. Biofuels* **6**, 51 (2013).
80. F. Taheripour, W. E. Tyner, Induced land use emissions due to first and second generation biofuels and uncertainty in land use emission factors. *Economic Res. Int.* **2013**, 1–12 (2013).
81. H. Valin *et al*., The land use change impact of biofuels consumed in the EU: Quantification of area and greenhouse gas impacts (2015). https://ec.europa.eu/energy/sites/ener/files/documents/Final%20Report_GLOBIOM_publication.pdf. Accessed 11 March 2019.